2013 European Control Conference (ECC)
July 17-19, 2013, Zürich, Switzerland.

Adaptive Output Tracking Control Design of a Gun Launched Micro Aerial Vehicle Based on Approximate Feedback Linearization

Adrien DROUOT, Edouard RICHARD, Mohamed BOUTAYEB, Michel ZASADZINSKI and Ali ZEMOUCHE

Abstract — **This paper considers the problem of controlling the position and the orientation of a Gun Launched Micro Aerial Vehicle - GLMAV - despite unknown aerodynamic efforts. The proposed approach overcomes the problem of gyroscopic coupling by taking advantage from the structure of the thrust mechanism, which is made of two counter rotating propellers. An adaptive linearizing controller is designed, allowing the trajectory tracking and the stabilization of the vehicle's position and orientation while the unknown aerodynamic efforts are estimated by means of an identifier. The overall process is shown to be stable for constant, or slowly time varying, aerodynamic efforts. However numerical simulations demonstrate the satisfying controller's performance even with non constant aerodynamic efforts.**

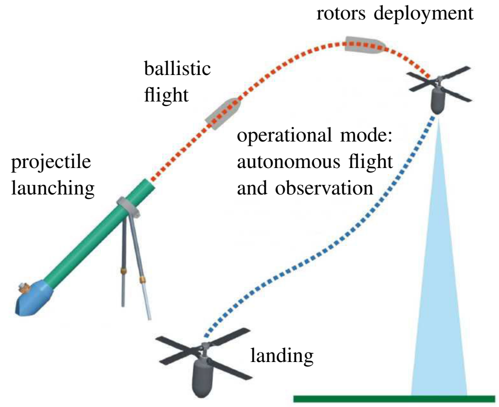

Fig. 1. Concept of the GLMAV

I. INTRODUCTION

The design of autonomous navigation strategies for Unmanned Micro Air Vehicles - UMAV - has now become a challenging research area, motivated by the recent technological advances in actuator miniaturization and embedded electronics [1], [6], [17], [30]. The UMAV main objective is to deport the human vision beyond the natural horizon, in order to accomplish risky missions in hostile environments. Therefore, these UMAV are of evident interest for both civil and military operations.

The GLMAV concept consists in bringing a UMAV very quickly onto the site where it begins to be operational by using the energy delivered by an external device. Thereby, the embedded energy is conserved for the autonomous flight only. The principle, illustrated in figure 1, is divided into three phases of flight. In the first one, the GLMAV, packaged into the projectile shell, is launched by a portable weapon and follows a ballistic trajectory to its apogee. In the second phase of flight, the projectile is transformed into a UMAV through the deployment of the rotors. Finally, the GLMAV fulfills its observation mission in the autonomous flight mode.

Therefore, the GLMAV is expected to perform hovering flights as well as aggressive flights despite possible wind perturbations. However, designing such autonomous navigation capabilities requires to handle some specific problems [23]. Indeed, the aerodynamic efforts that may apply on the vehicle are strongly nonlinear due to the atypical shape of the body and the very wide range of angle of attack. Moreover, this kind of aerial vehicle is unstable and its dynamics along the three axes are strongly coupled.

In the literature, both linear and nonlinear approaches have already been undertaken to control UMAV. The linear designs such as PID controllers [10], PD controllers [21] and cascaded PID controllers [16] disregard the input coupling and are effective application-oriented methods. The $\mathcal{H}_\infty$ control scheme [20], effective to cope with both model uncertainty and disturbance rejection, has also been succesfully tested on a wide range of UMAV [2], [5]. An interesting comparative study between several linear designs is given in [31]. But in those works, based on local linearization, the proof of convergence is not guaranteed when the vehicle leaves its flight domain.

More recently, interest has been focused on nonlinear globally stable control laws. However, designing detailed models of UMAV nonlinear dynamics is unsuitable for control design purposes [24]. Therefore, a simplified nonlinear model of the dynamics was introduced in [12], ignoring the input coupling. The resulting approximate model can be controlled via high gain designs, leading to a time scale separation between the cascaded systems [19], or backstepping designs, using dynamic extension of the thrust input [18], and dynamic inversion designs, leading to exact input-output linearization [12]. One of the difficulties in those designs is to deal with uncertain aerodynamic effects which may act on the vehicle. It has been overcome in [16], where the unwanted aerodynamic effects have been tabulated through intense wind tunnel tests, or in [9], which guarantees bounded tracking in the presence of parametric and model uncertainties.

This work is supported by the French National Research Agency under the number ANR 09 SECU.

A. Drouot, E. Richard, M. Boutayeb, M. Zasadzinski and A. Zemouche are with the Centre de Recherche en Automatique de Nancy, Université de Lorraine, CNRS UMR 7039, France - corresponding author: *adrien.drouot@univ-lorraine.fr*.

This paper focuses on an adaptive linearizing controller [26], [29], composed of a design based on approximate linearization connected to an identification structure. This approach involves coming up with a transformation of the nonlinear system into an equivalent linear system through a change of variables and a suitable control input. The question of modelling the aerodynamic effects is overthrown by considering them as unknown perturbations that act on the system. In [4] and [23], it was shown that an appropriate choice of adaptive filters in a backstepping process allows the estimation of unknown constant aerodynamic efforts. The main contribution of the paper is to introduce a control structure that handles unknown variable aerodynamic efforts.

II. SYSTEM MODELING

The GLMAV structure, based on coaxial contra-rotating rotors, is shown in figure 2. The mathematical model for the GLMAV can be derived using the physical laws of mechanics and aeromechanics. Early studies [7], [13] show that UMAV mathematical models can be divided into two submodels, i.e. a six degrees of freedom mechanical model coupled with an aerodynamic model. The main difficulty lies in the aerodynamic modelling which must be complete enough to accurately simulate the GLMAV dynamics and simple enough to develop future control laws for hovering and trajectory tracking.

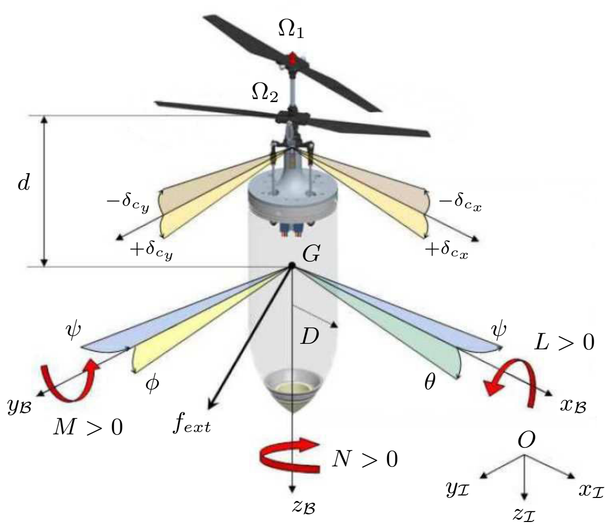

Fig. 2. Structure of the GLMAV

A. Mechanical model

To derive the mechanical model of the system, the Newton-Euler equations of motion of a rigid body have been employed. In particular, by considering an inertial frame $\{O, x_{\mathcal{I}}, y_{\mathcal{I}}, z_{\mathcal{I}}\}$ and a coordinate frame $\{G, x_{\mathcal{B}}, y_{\mathcal{B}}, z_{\mathcal{B}}\}$ attached to the body of the vehicle. The dynamical model of the aircraft with respect to the inertial frame is described by:

$$\begin{aligned} \dot{p} &= v \\ m\dot{v} &= R_\eta f \\ J\dot{\Omega} &= -\Omega \times J\Omega + \Gamma \end{aligned} \tag{1}$$

where p and v represent, respectively, the position and the velocity of the center of mass, m the vehicle total mass which is assumed constant, J the diagonal inertia matrix, Ω the angular velocity expressed in the body frame, f and Γ the vector of forces and torques applied to the vehicle expressed in the body frame and R_η the rotation matrix relating the two reference frames. The rotation matrix R_η can be parameterized by means of the roll ϕ, pitch θ and yaw ψ obtaining:

$$R_\eta = \begin{bmatrix} c_\theta c_\psi & s_\phi s_\theta c_\psi - c_\phi s_\psi & c_\phi s_\theta c_\psi + s_\phi s_\psi \\ c_\theta s_\psi & s_\phi s_\theta s_\psi + c_\phi c_\psi & c_\phi s_\theta s_\psi - s_\phi c_\psi \\ -s_\theta & s_\phi c_\theta & c_\phi c_\theta \end{bmatrix}. \tag{2}$$

The attitude kinematics is given by:

$$\dot{\eta} = Q_\eta \Omega \qquad \text{with} \quad Q_\eta = \begin{bmatrix} 1 & s_\phi t_\theta & c_\phi t_\theta \\ 0 & c_\phi & -s_\phi \\ 0 & s_\phi / c_\theta & c_\phi / c_\theta \end{bmatrix} \tag{3}$$

having denoted by, for convenience, $\eta = \begin{bmatrix}\phi & \theta & \psi\end{bmatrix}^T$, $c_\varrho = \cos\varrho$, $s_\varrho = \sin\varrho$ and $t_\varrho = \tan\varrho$.

B. Aerodynamic model

The aerodynamic model focuses on the loads generated by the coaxial rotors and the cyclic swashplate incidence angles. The gyroscopic moments induced by the contrarotating rotors are neglected because they offset each other assuming that the speed differential is virtually zero or not large enough to induce a significant gyroscopic moment. Further explanations on the aerodynamic modeling can be found in [11].

1) Forces generated by the coaxial rotors The thrust is the main force generated by the two rotors. The upper rotor contributes only to the vertical thrust whereas the lower rotor, which generates both a vertical thrust and two lateral forces due to the swashplate incidence angles. The total force T generated by the coaxial rotors is:

$$T = \begin{bmatrix} T_x \\ T_y \\ T_z \end{bmatrix} = \begin{bmatrix} -\beta \sin\delta_{c_y} \cos\delta_{c_x} \Omega_2^2 \\ -\beta \sin\delta_{c_x} \Omega_2^2 \\ \alpha\Omega_1^2 + \beta \cos\delta_{c_x} \cos\delta_{c_y} \Omega_2^2 \end{bmatrix} \tag{4}$$

where α and β are the rotors aerodynamic coefficients, Ω_1 and Ω_2 the rotors rotation speeds and δ_{c_x} and δ_{c_y} the swashplate incidence angles.

2) Forces acting on the body Due to the numerous interactions existing between the GLMAV and its environment, several aerodynamic forces, such as the form drag, the momentum drag and the friction drag, should be modelled. However, the net force of these aerodynamic effects and its point of application are hard to determine because of its dependence on the wind, which is unpredictable. This is why the net force will be denoted by f_{ext} in the body frame and by F_{ext} in the inertial frame.

The weight force component f_w acting on the GLMAV is written as:

$$f_w = mg \begin{bmatrix} -\sin\theta \\ \sin\phi\cos\theta \\ \cos\phi\cos\theta \end{bmatrix} = R_\eta^T \begin{bmatrix} 0 \\ 0 \\ mg \end{bmatrix}. \tag{5}$$

By adding the different force vectors, the three components X, Y and Z of the total force vector f applied to the GLMAV are:

$$f = \begin{bmatrix} X & Y & Z \end{bmatrix}^T = T + f_w + f_{ext}. \tag{6}$$

3) Moments induced by the coaxial rotors A torque about the longitudinal or lateral axis may be produced via differentially pitching the swashplate incidence angles δ_{c_x} and δ_{c_y}. The torque on the vertical axis is induced by the rotation speed difference between the two rotors. The roll, pitch and yaw moments are then given by:

$$\tau = \begin{bmatrix} \tau_L \\ \tau_M \\ \tau_N \end{bmatrix} = \begin{bmatrix} -d\beta \sin \delta_{c_x} \Omega_2^2 \\ d\beta \sin \delta_{c_y} \cos \delta_{c_x} \Omega_2^2 \\ \gamma_1 \Omega_1^2 + \gamma_2 \Omega_2^2 \end{bmatrix} \tag{7}$$

where d is the distance between the center of gravity and the lower rotor center of rotation and γ_1 and γ_2 are the yaw aerodynamic coefficients.

4) Moments acting on the body The external forces f_{ext} apply at a point difficult to determine, depending on the incidence of the vehicule in the air flow and on the air flow itself. However, because of the symmetrical property of the GLMAV, it is assumed that this point is located somewhere on the $z_{\mathcal{B}}$ axis but different from the center of gravity. Therefore a resultant moment M_{ext} exists and is nonzero, except on the $z_{\mathcal{B}}$ axis.

The weight force component f_w, because it applies at the center of gravity of the GLMAV, does not induce any moment.

By adding the different moment vectors, the three components L, M and N of the total moment vector Γ applied to the GLMAV are:

$$\Gamma = \begin{bmatrix} L & M & N \end{bmatrix}^T = \tau + M_{ext}. \tag{8}$$

The GLMAV is defined as a nonlinear system governed by the four control inputs Ω_1 and Ω_2, the upper and lower rotor rotational speeds, and δ_{c_x} and δ_{c_y}, the cyclic swashplate incidence angles along the roll and pitch axes.

III. CONTROL DESIGN

In this section, an adaptive controller is developped for the GLMAV using feedback linearization techniques [26], [29]. This approach involves coming up with a transformation of the nonlinear system into an equivalent linear system through a change of variables and a suitable control input. The control structure is completed by an observer-based identifier which estimates the unknown aerodynamic effects that may arise.

The objective of the controller is to asymptotically track the desired longitudinal, lateral, vertical and heading time references $x_d(t)$, $y_d(t)$, $z_d(t)$ and $\psi_d(t)$. The reference signals are assumed to be known arbitrary time profiles with the only restrictions dictated by the functional controllability of the system, by the fulfillment of the flight envelope constraints and of physical constraints on the control inputs. In the proposed design, it is assumed that all the internal states are accessible for control purpose. Furthermore the initial states are supposed to belong to any compact set with the only restriction that the paraxial approximation can be used.

A. Model simplification

In order to simplify the synthesis of the control law, a certain number of approximations shall be considered. In particular the lateral forces T_x and T_y will be assumed negligible compared to the contribution of main thrust T_z. The system (1), with $\varkappa = 1/m$ becomes:

$$\begin{aligned} \ddot{p} = \dot{v} = \varkappa T_z R_\eta e_3 + g e_3 + \varkappa F_{ext} \\ J\dot{\Omega} = -\Omega \times J\Omega + \tau + M_{ext} \end{aligned} \tag{9}$$

where F_{ext} and M_{ext} represent, respectively, external force and torque applied to the GLMAV which will be assumed constant. These unknown vectors will be estimated in the control law by $\hat{F}_{ext}$ and $\hat{M}_{ext}$. The estimation errors between the real external forces and torques and the estimated ones will denoted by $\tilde{F}_{ext}$ and $\tilde{M}_{ext}$.

By considering small enough the swashplate incidence angles, the paraxial approximation, meaning that $\cos \varpi = 1$ and $\sin \varpi = \varpi$, can be used. Hence the four control inputs Ω_1, Ω_2, δ_{c_x} and δ_{c_y}, from (4) and (7), are given by:

$$\begin{aligned} \Omega_1^2 &= \left(T_z - \beta \Omega_2^2\right) / \alpha \\ \Omega_2^2 &= \left(\alpha \tau_N - \gamma_1 T_z\right) / \left(\alpha \gamma_2 - \beta \gamma_1\right) \\ \delta_{c_x} &= -\tau_L / d\beta \Omega_2^2 \\ \delta_{c_y} &= \tau_M / d\beta \Omega_2^2 \end{aligned} \tag{10}$$

with T_z and τ the new control inputs to be determined.

B. Approximate linearization technique

The approximate linearization process [26], [29] is now applied to our system (9). The objective of the process is to obtain an equation such as:

$$\begin{aligned} \left(y^{(\gamma)} - y_d^{(\gamma)}\right) + \alpha_{\gamma-1} \left(y^{(\gamma-1)} - y_d^{(\gamma-1)}\right) + \dots \\ \dots + \alpha_0 \left(y - y_d\right) = 0 \end{aligned} \tag{11}$$

where $y(t)$ has to track a given $y_d(t)$ and where $\alpha_0, \dots, \alpha_{\gamma-1}$ are chosen such that:

$$s^\gamma + \alpha_{\gamma-1} s^{\gamma-1} + \dots + \alpha_0 = 0 \tag{12}$$

is a Hurwitz polynomial. The integer γ is called the *strong relative degree* of the system (9). It is the number of times the output has to be differentiated before the input appears explicitly. As mentionned before, the objective is to track some desired position and heading time references. Therefore, the outputs p and ψ need to be differentiated until the control inputs T_z and τ appear.

From (9), the two first derivatives of p are easily computed:

$$\dot{p} = v \tag{13}$$

$$\ddot{p} = \varkappa T_z R_\eta e_3 + g e_3 + \varkappa F_{ext}. \tag{14}$$

As T_z is a physical system input, it is tempting to stop the process at this step. However, following this approach leads to a time-scale separation of the system dynamics [28]. That approach would be advantageous in hover control to ensure that this part of the system is more firmly controlled than other system states. However, in more general trajectories a time-scale separation imposed in the dynamics at this stage may lead to significant robustness problems. In particular, derivatives of the control T_z enter into the remaining dynamics of the system and aggressive control may lead to extreme ill-conditioning of the remaining control problem [18]. An alternative strategy will be to take a dynamic extension of the control T_z [8]. Consider the system of two integrators, cascaded to the primary thrust input:

$$\dot{T}_z = \bar{T}_z \qquad \text{and} \qquad \dot{\bar{T}}_z = \bar{\bar{T}}_z. \tag{15}$$

The system input T_z and its derivative $\bar{T}_z$ are now viewed as internal states of the controller. The new system inputs are now τ and $\bar{\bar{T}}_z$ all of which enter the system with the same dynamic order of four. This approach offers a compromise between the different control objectives of the trajectory tracking problem.

The differentiation of (14) with respect to time is given by:

$$p^{(3)} = \varkappa \bar{T}_z R_\eta e_3 + \varkappa T_z R_\eta \tilde{\Omega} e_3 \tag{16}$$

with $R_\eta \tilde{\Omega} = \dot{R}_\eta$ and where $\tilde{\Omega}$ is the skew symmetric matrix of the vector Ω. Let's remind that F_{ext} is assumed constant, so $\dot{F}_{ext} = 0$.

The differentiation of (16) leads to[1]:

$$\begin{aligned} p^{(4)} = \varkappa \bar{\bar{T}}_z R_\eta e_3 + 2\varkappa \bar{T}_z R_\eta \tilde{\Omega} e_3 \\ + \varkappa T_z R_\eta \tilde{\Omega}^2 e_3 - \varkappa T_z R_\eta \tilde{e}_3 \dot{\Omega} \end{aligned} \tag{17}$$

where $\tilde{e_3}$ is the skew symmetric matrix of the vector e_3.

From (3), the first derivative of ψ is easily computed:

$$\dot{\psi} = e_3^T \dot{\eta} = e_3^T Q_\eta \Omega. \tag{18}$$

Differentiating (18) with respect to time leads to:

$$\ddot{\psi} = e_3^T \dot{Q}_\eta \Omega + e_3^T Q_\eta \dot{\Omega}. \tag{19}$$

According to (9), (17) and (19) can be rewritten as:

$$\begin{aligned} p^{(4)} = \varkappa \bar{\bar{T}}_z R_\eta e_3 + 2\varkappa \bar{T}_z R_\eta \tilde{\Omega} e_3 \\ + \varkappa T_z R_\eta \tilde{\Omega}^2 e_3 - \varkappa T_z R_\eta \tilde{e}_3 J^{-1} \tau \\ - \varkappa T_z R_\eta \tilde{e}_3 J^{-1} \left(-\Omega \times J\Omega + M_{ext} \right) \end{aligned} \tag{20}$$

and:

$$\begin{aligned} \ddot{\psi} = e_3^T \dot{Q}_\eta \Omega + e_3^T Q_\eta J^{-1} \tau \\ + e_3^T Q_\eta J^{-1} \left(\Omega \times J\Omega + M_{ext} \right). \end{aligned} \tag{21}$$

Applying the linearization process (11) to the output p leads to:

$$\begin{aligned} &\Big(\varkappa \bar{\bar{T}}_z R_\eta e_3 + 2\varkappa \bar{T}_z R_\eta \tilde{\Omega} e_3 + \varkappa T_z R_\eta \tilde{\Omega}^2 e_3 \\ &- \varkappa T_z R_\eta \tilde{e}_3 J^{-1} \left(-\Omega \times J\Omega + M_{ext} \right) \\ &- \varkappa T_z R_\eta \tilde{e}_3 J^{-1} \tau - p_d^{(4)} \Big) \\ &+ \alpha_3 \left(\varkappa \bar{T}_z R_\eta e_3 + \varkappa T_z R_\eta \tilde{\Omega} e_3 - p_d^{(3)} \right) \\ &+ \alpha_2 \left(\varkappa T_z R_\eta e_3 + g e_3 + \varkappa F_{ext} - \ddot{p}_d \right) \\ &+ \alpha_1 \left(v - \dot{p}_d \right) + \alpha_0 \left(p - p_d \right) = 0 \end{aligned} \tag{22}$$

[1]Recall that for any vector u, v: $\tilde{u}v = u \times v = -v \times u = -\tilde{v}u$

and its application to the output ψ leads to:

$$\begin{aligned} &\Big(e_3^T \dot{Q}_\eta \Omega + e_3^T Q_\eta J^{-1} \left(-\Omega \times J\Omega + M_{ext} \right) \\ &+ e_3^T Q_\eta J^{-1} \tau - \ddot{\psi}_d \Big) \\ &+ \beta_1 \left(e_3^T Q_\eta \Omega - \dot{\psi}_d \right) + \beta_0 \left(\psi - \psi_d \right) = 0. \end{aligned} \tag{23}$$

Therefore, the control signals $\bar{\bar{T}}_z$ and τ are given by:

$$\begin{bmatrix} \tau \\ \bar{\bar{T}}_z \end{bmatrix} = \underbrace{\begin{bmatrix} -\varkappa T_z R_\eta \tilde{e}_3 J^{-1} & \varkappa R_\eta e_3 \\ e_3^T Q_\eta J^{-1} & 0 \end{bmatrix}^{-1}}_{H^{-1}} \begin{bmatrix} A \\ B \end{bmatrix} \tag{24}$$

where:

$$\begin{aligned} A = p_d^{(4)} - 2\varkappa \bar{T}_z R_\eta \tilde{\Omega} e_3 - \varkappa T_z R_\eta \tilde{\Omega}^2 e_3 \\ + \varkappa T_z R_\eta \tilde{e}_3 J^{-1} \left(-\Omega \times J\Omega + M_{ext} \right) \\ - \alpha_3 \left(\varkappa \bar{T}_z R_\eta e_3 + \varkappa T_z R_\eta \tilde{\Omega} e_3 - p_d^{(3)} \right) \\ - \alpha_2 \left(\varkappa T_z R_\eta e_3 + g e_3 + \varkappa F_{ext} - \ddot{p}_d \right) \\ - \alpha_1 \left(v - \dot{p}_d \right) - \alpha_0 \left(p - p_d \right) \end{aligned} \tag{25}$$

and:

$$\begin{aligned} B = \ddot{\psi}_d - e_3^T \dot{Q}_\eta \Omega \\ - e_3^T Q_\eta J^{-1} \left(-\Omega \times J\Omega + M_{ext} \right) \\ - \beta_1 \left(e_3^T Q_\eta \Omega - \dot{\psi}_d \right) - \beta_0 \left(\psi - \psi_d \right). \end{aligned} \tag{26}$$

It is obvious that the matrix in (24) must be invertible so that the procedure is successful. There are only two configurations in which this is not the case. The first one is a configuration where the main thrust T_z crosses 0. The second one is a configuration where the GLMAV has overturned. Those conditions are straightforward when one sees the expression of the determinant of H:

$$\det(H) = -\frac{1}{m^3} \frac{1}{J_{xx} J_{yy} J_{zz}} T_z^2 \frac{\cos\phi}{\cos\theta}. \tag{27}$$

From (25) and (26), one can easily notice that an explicit expression is required for F_{ext} and M_{ext}. As they are unknown, due to their dependence on the wind, an identifier has to be used.

C. Identifier structure

Consider the system:

$$\dot{x} = f(x, \zeta) + g(x, \zeta) u \tag{28}$$

where $x \in \mathbb{R}^n$ denotes the state, $u \in \mathbb{R}$ is the control input to the system and $\zeta \in \mathbb{R}^p$ is a constant vector of unknown parameters. The state function f and the input function g are assumed to be smooth vector fields on $\mathbb{R}^n$. Further, let $f(x, \zeta)$ and $g(x, \zeta)$ have the form:

$$f(x, \zeta) = f_0(x) + \sum_{i=1}^{p} f_i(x) \zeta_i \tag{29}$$

$$g(x, \zeta) = g_0(x) + \sum_{i=1}^{p} g_i(x) \zeta_i. \tag{30}$$

Here ζ_i, $i = 1, \dots, p$, are unknown parameters which appear linearly and the smooth vector fields $f_0(x)$, $f_i(x)$, $g_0(x)$ and $g_i(x)$ are known. Let the regressor be:

$$w^T(x,u) = [f_1(x) + g_1(x)u, \ldots, f_p(x) + g_p(x)u], \quad (31)$$

then (28) can be written as:

$$\dot{x} = w_0(x,u) + w^T(x,u)\zeta \quad (32)$$

where:

$$w_0(x,u) = f_0(x) + g_0(x)u. \quad (33)$$

To estimate the unknown parameters, the following identifier system is used:

$$\begin{aligned} \dot{\hat{x}} &= A(\hat{x} - x) + w_0(x,u) + w^T(x,u)\hat{\zeta} \\ \dot{\hat{\zeta}} &= -w(x,u)P(\hat{x} - x). \end{aligned} \quad (34)$$

where $\hat{x}$ is the observer state, $\hat{\zeta}$ is the estimated parameter, $A \in \mathbb{R}^{n\times n}$ is a Hurwitz matrix and $P \in \mathbb{R}^{n\times n} > 0$ is a solution to the Lyapunov equation:

$$A^T P + PA = -Q, \qquad Q > 0. \quad (35)$$

This identifier structure is reminiscent of one proposed in [15] and [27]. Defining $e = \hat{x} - x$ as the observer state error, and $\varepsilon = \hat{\zeta} - \zeta$ as the parameter error, and assuming ζ to be constant but unknown, then the following error system can be stated:

$$\begin{aligned} \dot{e} &= Ae + w^T(x,u)\varepsilon \\ \dot{\varepsilon} &= -w(x,u)Pe \end{aligned} \quad (36)$$

The proof of stability of the observer-based identifier is a standard Lyapunov argument on the function:

$$V(e,\varepsilon) = \frac{1}{2}e^T Pe + \frac{1}{2}\varepsilon^T\varepsilon \quad (37)$$

which is decreasing along the trajectories of (36); thereby establishing bounded e and ε. However, to prove that $e \to 0$ as $t \to \infty$, it must be shown that e is uniformly continuous or, alternatively, that $\dot{e}$ is bounded. This in turn needs w to be bounded as well. And it was shown in [25] that if the system is bounded-input bounded-state stable with bounded input, then w is bounded. Furthermore, as is standard in literature [3], [14], [22], one can conclude from (36) that e and ε both converge exponentially to zero if w is sufficiently rich, i.e. $\exists\ \rho_1,\ \rho_2,\ \delta > 0$ such that:

$$\rho_1 I \leqslant \int_s^{s+\delta} ww^T dt \leqslant \rho_2 I, \quad (38)$$

also known as a persistently exciting condition.

The application of the identification technique to our system is straightforward by taking:

$$w_0(x,u) = \begin{bmatrix} v \\ \varkappa T_z R_\eta e_3 + ge_3 \\ Q_\eta \Omega \\ J^{-1}(-\Omega \times J\Omega + \tau) \end{bmatrix}, \quad (39)$$

$$w^T(x,u) = \begin{bmatrix} 0_{3\times3} & 0_{3\times3} \\ \varkappa I_{3\times3} & 0_{3\times3} \\ 0_{3\times3} & 0_{3\times3} \\ 0_{3\times3} & J^{-1} \end{bmatrix} \quad \text{and:} \quad \zeta = \begin{bmatrix} F_{ext} \\ M_{ext} \end{bmatrix}. \quad (40)$$

IV. SIMULATION RESULTS

Some simulations were performed on the complete model, with physical parameters given in [4], including the terms neglected in the control design. The initial conditions are those expected at the beginning of the third phase of flight. Hence the roll, pitch and yaw angles, such as the position in the horizontal plane, are set to 0 while the initial altitude is fixed to $z_0 = 110\ m$. The trajectories to be tracked are composed of a stream of steps, which is typically what will be asked during the real flights.

The parameters $\alpha_i,\ i = 0,1,2,3$, and $\beta_j,\ j = 0,1$, are chosen such that the eigenvalues of the closed-loop system are located at - 2. That is:

$$\begin{aligned} \alpha_0 = 16, \quad \alpha_1 = 32, \quad \alpha_2 = 24, \quad \alpha_3 = 8 \\ \beta_0 = 4, \quad \beta_1 = 4 \end{aligned} \quad (41)$$

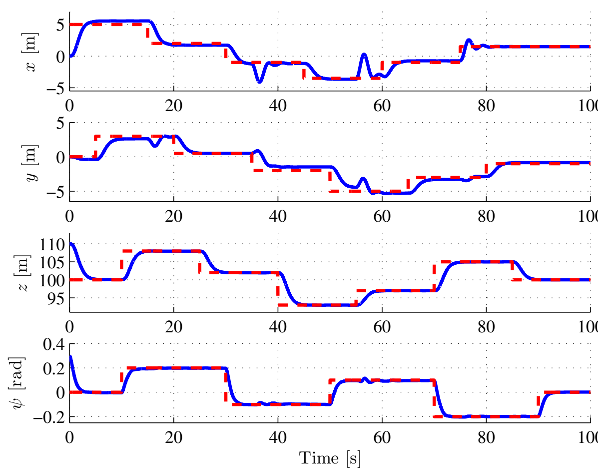

Fig. 3. Output signals x, y, z and ψ (solid blue lines) and reference signals (dashed red lines)

Figure 3 shows the evolution of the vehicle's position and orientation during its flight, in presence of variable wind gusts (the results with piecewise constant wind gusts are not presented here for reason of space). The unknown efforts arising from those gusts are estimated by the identifier and are shown in figure 4. One can see on this figure that the estimated efforts convergence to their real value relatively fast. Figure 5 shows the bounded behavior of the control inputs. From these figures, it is clear that the designed controller, with the appropriate identifier, succeeds in reaching the desired position despite unknown aerodynamic efforts. However, the success in tracking the desired trajectories strongly relies on how fast the wing gusts arise. Indeed, as long as the dynamics of the observer-based identifier is faster than the dynamics of the wind gusts, the tracking will be done properly. Otherwise, the performance in identifying the wind gust, and thus in tracking, will be significantly damaged.

V. CONCLUSION

In this paper, a design of a Gun Launched Micro Aerial Vehicle was presented. Its dynamic model, suitable for

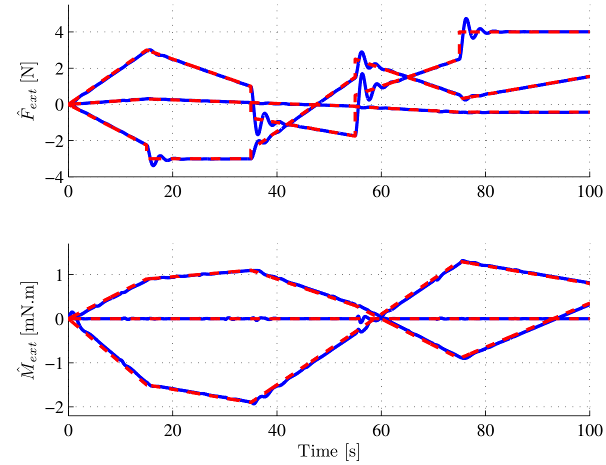

Fig. 4. Estimation of the unknown effort $\hat{F}_{ext}$ and torque $\hat{M}_{ext}$ (solid blue lines) and their true values (dashed red lines)

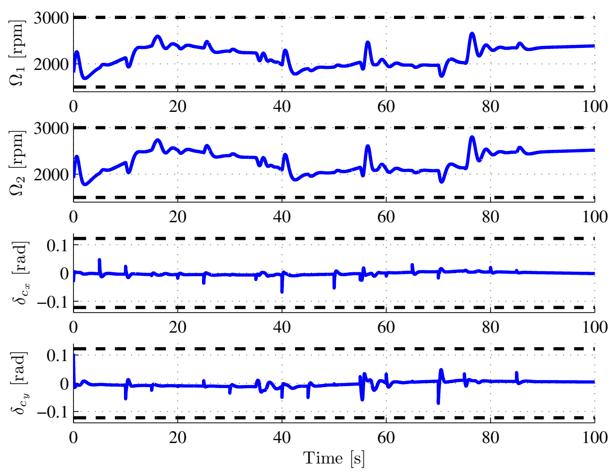

Fig. 5. Control signals Ω_1, Ω_2, δ_{c_x} and δ_{c_y}

control purposes, was proposed including some aerodynamic effects which are considered as unknown perturbing terms. The observer-based identifier linked to controller allows the GLMAV to be stabilized to a given position and orientation despite these perturbations. Numerical simulations are provided to illustrate the good performance of the control law. In future work, the designed control structure will be implemented and tested on a model of GLMAV.

References

[1] P. Castillo, R. Lozano, and A.E. Dzul. *Modelling and Control of Mini-Flying Machines*. Springer, 2005.

[2] M. La Civita, G. Papageorgiou, W.C. Messner, and T. Kanade. Design and Flight Testing of an $\mathcal{H}_\infty$ Controller for a Robotic Helicopter. *Journal of Guidance, Control, and Dynamics*, pages 485–494, 2006.

[3] Y.L. Dong and S.W. Mei. Adaptive Observer for a Class of Nonlinear Systems. *Acta Automatica Sinica*, 33(10):1081–1084, 2007.

[4] A. Drouot, E. Richard, and M. Boutayeb. An Approximate Backstepping Based Trajectory Tracking Control of a Gun Launched Micro Aerial Vehicle in Crosswind. *Journal of Intelligent and Robotic Systems*, 70(1):133–150, 2013.

[5] J. Gadewadikar, F. Lewis, K. Subbarao, and B. Chen. Structured $\mathcal{H}_\infty$ Command and Control-Loop Design for Unmanned Helicopters. *Journal of Guidance, Control and Dynamics*, 31:1093–1102, 2008.

[6] R. Ganguli. Survey of Recent Developments in Rotorcraft Design Optimization. *Journal of Aircraft*, 41(3):493–510, 2004.

[7] P. Gnemmi, A. Koehl, B. Martinez, S. Changey, and S. Theodoulis. Modeling and Control of Two GLMAV Hover-Flight Concepts. *Proceedings of the European Micro Aerial Vehicle Conference*, 2009.

[8] A. Isidori. *Nonlinear Control Systems: An Introduction*. Springer, 1989.

[9] A. Isidori, L. Marconi, and A. Serrani. Robust Nonlinear Motion Control of a Helicopter. *IEEE Transactions on Automatic Control*, 48:413–426, 2003.

[10] H.J. Kim and D.H. Shim. A Flight Control System for Aerial Robots: Algorithms and Experiments. *Control Engineering Practice*, 11:1389–1400, 2003.

[11] A. Koehl, H. Rafaralahy, M. Boutayeb, and B. Martinez. Modeling and Identification of a Launched Micro Air Vehicle: Design and Experimental Results. *Proceedings of the AIAA Modeling and Simulation Technologies Conference and Exhibit*, 2010.

[12] T.J. Koo and S. Sastry. Output Tracking Control Design of a Helicopter Model Based on Approximate Linearization. *Proceedings of the 37th IEEE Conference on Decision and Control*, 4:3635–3640, 1998.

[13] R. Krashanitsa, G. Platanitis, D. Silin, and S. Shkarayev. Aerodynamics and Controls Design for Autonomous Micro Air Vehicles. *Proceedings of the AIAA Atmospheric Flight Mechanics Conference and Exhibit*, 2006.

[14] G. Kreisselmeier. Adaptive Observers with Exponential Rate of Convergence. *IEEE Transactions on Automatic Control*, 22:2–8, 1977.

[15] P. Kudva and K.S. Narendra. Synthesis of an Adaptive Observer using Lyapunov's Direct Method. *International Journal of Control*, 18:1201–1210, 1973.

[16] L. Lipera, J.D. Colbourne, M.B. Tischler, M. Hossein Mansur, M.C. Rotkowitz, and P. Patangui. The Micro Craft iSTAR Micro Air Vehicle: Control System Design and Testing. *Proceedings of the 57th Annual Forum of the American Helicopter Society*, pages 1–11, 2001.

[17] R. Lozano. *Unmanned Aerial Vehicles Embedded Control*. John Wiley-ISTE Ltd, 2010.

[18] R. Mahony and T. Hamel. Robust Trajectory Tracking for a Scale Model Autonomous Helicopter. *International Journal of Robust and Nonlinear Control*, 14(12):1035–1059, 2004.

[19] R. Mahony, T. Hamel, and A. Dzul. Hover Control via Lyapunov Control for an Autonomous Model Helicopter. *Proceedings of the 38th IEEE Conference on Decision and Control*, 4:3490–3495, 1999.

[20] D. McFarlane and K. Glover. A Loop-Shaping Design Procedure using $\mathcal{H}_\infty$ Synthesis. *IEEE Trans. on Automatic Control*, 37:759–769, 1992.

[21] B. Mettler. *Identification Modeling and Characteristics of Miniature Rotorcraft*. Kluwer Academic Publishers, 2003.

[22] A.P. Morgan and K.S. Narendra. On the Uniform Asymptotic Stability of Certain Linear Nonautonomous Differential Equations. *SIAM Journal on Control and Optimization*, 15(1):5–24, 1977.

[23] J. M. Pflimlin, P. Soueres, and T. Hamel. Position Control of a Ducted Fan VTOL UAV in Crosswind. *International Journal of Control*, 80(5):666–683, 2007.

[24] R.W. Prouty. *Helicopter Performance, Stability and Control*. Krieger Publishing Company, 1995.

[25] S. Sastry and M. Bodson. *Adaptive Control: Stability, Convergence, and Robustness*. Prentice-Hall, Inc, 1989.

[26] S.S. Sastry and A. Isidori. Adaptive Control of Linearizable Systems. *IEEE Transactions on Automatic Control*, 34:1123–1131, 1989.

[27] S. Sheikholeslam. Observer-Based Parameter Identifiers for Nonlinear Systems with Parameter Dependencies. *IEEE Transactions on Automatic Control*, 40(2):382–387, 1995.

[28] A.R. Teel. A Nonlinear Small Gain Theorem for the Analysis of Control Systems with Saturation. *IEEE Transactions on Automatic Control*, 41:1256–1270, 1996.

[29] A.R. Teel, R. Kadiyala, P. Kokotovic, and S.S. Sastry. Indirect Techniques for Adaptive Input-Output Linearization of Non-Linear Systems. *International Journal of Control*, 53:193–222, 1991.

[30] K. P. Valavanis. *Advances in Unmanned Aerial Vehicles: State of the Art and the Road to Autonomy*. Springer, 2007.

[31] M.F. Weilenmann, U. Christen, and H.P. Geering. Robust Helicopter Position Control at Hover. *Proceedings of the American Control Conference*, 3:2491–2495, 1994.